

Hearing Protection for Bone-Conducted Sound

Anthony J. Dietz, Ph.D.
B. Scott May, Ph.D., Darin A. Knaus, Ph.D., Harold P. Greeley
Creare Incorporated
PO Box 71, Hanover, NH 03755, USA
ajd@creare.com

ABSTRACT

The high-noise environments in and around modern military jet aircraft can impair voice communications and cause permanent damage to the hearing of pilots and maintenance crews if adequate hearing protection is not worn. With external noise levels of some aircraft approaching 150 dBA, adequate hearing protection must provide better than 50 dB of attenuation. In order to reach such a high level of attenuation, sound-transmission routes that bypass the ear canal must be attenuated in addition to the ear canal transmission routes. These bone- and tissue-conduction paths limit the maximum attenuation that can be achieved, even if all air-conducted sound in the ear canal were eliminated.

An investigation of bypass sound transmission mechanisms is presented. The aim of this investigation was to characterise the transmission levels of bypass sound to the cochlea and to determine the effectiveness of different hearing protection components in attenuating this sound. Measurements were made with a head simulator as well as with human subjects.

In order to make detailed measurements of the vibration of skull bones in an intense sound field, we developed a head simulator. The simulator was built from a human skull, with silicon gel used to model internal organs and silicon and latex used to model the skin. Accelerometers attached to the skull bones were used to measure the skull vibration response. Mechanical point impedance measurements on the simulator were compared to results reported in the literature for humans, cadavers, and skulls. Reasonable agreement with these results served to validate the simulation. The relationship between skull vibration measured on the skull simulator and bone-conducted sound at the cochlea of a human subject was determined by comparing mechanical point impedance measurements recorded from the skull simulator and from human subjects, with the latter including psycho-acoustic responses. The effect of different hearing protection components on skull vibration and on the attenuation perceived by human subjects was also measured. Finally, the attenuation limits for bypass sound routes through the head and through the torso were determined.

The response of the head simulator in a sound field peaked in the 1 to 3 kHz frequency range, which is where the bone-conducted limit to hearing protection attenuation is at a minimum. The bypass sound levels measured on human subjects also increased in this frequency range. The performance of different hearing protection components including ear muffs, helmets, goggles, and face shields was measured on the head simulator and on human subjects, and the results are reported. General guidance concerning the design of devices for providing protection against bypass sound transmission is given. Finally, the need for additional protection of the torso is discussed.

Dietz, A.J.; May, B.S.; Knaus, D.A.; Greeley, H.P. (2005) Hearing Protection for Bone-Conducted Sound. In *New Directions for Improving Audio Effectiveness* (pp. 14-1 – 14-18). Meeting Proceedings RTO-MP-HFM-123, Paper 14. Neuilly-sur-Seine, France: RTO.
Available from: <http://www.rto.nato.int/abstracts.aps>.

1.0 INTRODUCTION

In situations where personnel are required to work in extreme noise environments, the protection provided by hearing protection devices (HPDs) is often insufficient. Even if the sound transmitted to the ear canal was completely attenuated, the sound reaching the cochlea via bone conduction transmission paths that bypass the HPD can still be loud enough to cause hearing damage. Improved understanding of these bypass sound transmission paths will lead to improved hearing protection, allowing safe exposure to high sound levels.

1.1 Extreme Noise Environments

Military jet aircraft operating at full afterburner can produce sound levels in the vicinity of 150 dBA. Crews working in close proximity to these aircraft need hearing protection that allows them to complete a work shift without exceeding the allowable exposure limit. With a hearing conservation limit of 85 dBA for eight hours with a 3 dB exchange rate and assuming sixty, thirty-second takeoff or landing events in a work shift, the allowable noise exposure during each event is 97 dBA. For events approaching sound levels of 150 dBA, hearing protection providing attenuation in excess of 50 dB is required.

1.2 Hearing Protection Limits

Bone conduction transmission paths limit the maximum attenuation that can be achieved with double hearing protection (earplugs and earmuffs). For example, in the 2 kHz octave band, Real Ear Attenuation at Threshold (REAT) measurements by Berger et al. (2003) gave a mean attenuation of 37 dB for deeply inserted foam earplugs and 36 dB for earmuffs. However, the attenuation measured with both earmuffs and earplugs in place was only 41 dB, far less than would be expected from the combined component attenuation values. The attenuation was limited by transmission paths that bypassed the hearing protection devices. When a third level of protection was introduced in the form of a helmet, the total attenuation increased to 49 dB.

1.3 Bone Conduction Transmission Paths

The various transmission paths that bypass the attenuation provided by double hearing protection devices are collectively known as bone conduction transmission paths. Four primary bone conduction transmission paths have been identified in the numerous research studies on this phenomenon (e.g., Tonndorf et al. 1966; Sohmer et al. 2000). These are: (1) inertial movement of the ossicular bones relative to the skull at low frequencies, (2) distortion of the temporal bone and cochlear shell at high frequencies, (3) osseotympanic transmission of sound radiated from the walls of an occluded ear canal, and (4) sound conduction via fluid pathways connecting the cochlea to the brain cerebrospinal fluid. The resultant sound level at the cochlea is a frequency-dependent vector sum of the contributions from each of these transmission mechanisms.

A graphical representation of the various transmission paths is shown in Figure 1. The ability of hearing protection devices to attenuate the sound level at the cochlea will depend on their effectiveness against each of these transmission paths. Earplugs are effective against air-conducted sound transmission and against bone-conducted sound transmitted to the ear canal. Earmuffs are effective against air-conducted sound and provide limited shielding of the head. A helmet further shields the head, attenuating both air- and bone-conducted sound. Finally, even if the head is completely shielded, a body conduction path remains. In order to design effective hearing protection for extreme noise environments, the relative limits between the air, head, and body conduction transmission paths must be known.

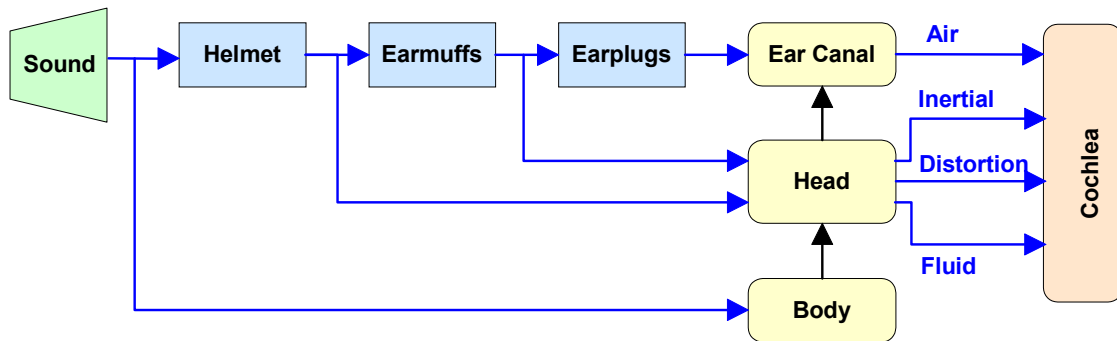


Figure 1. Transmission of Sound to the Cochlea.

1.4 Previous Studies

Previous studies have focused on the vibration response of the head to mechanical driving point forcing and on the psycho-acoustic perception of the bone-conducted sound generated by such forcing. Studies of the vibration response of the head have primarily reported impedance measurements. Smith and Suggs (1976) measured the mechanical impedance to point forcing of human heads. Hakansson et al. (1986) measured the mechanical impedance at the mastoid with and without skin penetration, and Stenfelt and Hakansson (1999) measured the impedance at the teeth. Impedance measurements have also been made on monkeys and cadavers (Stalnaker et al. 1971) and on dry skulls (Stenfelt et al. 2000). There are significant differences in both the magnitude and frequency dependence of the impedance data reported. No studies of the vibration response of a head in a sound field were located.

A number of studies on bone-conducted sound have been concerned with identifying the relative thresholds or limits of bypass sound transmission through the head and body. Berger et al. (2003) compiled an extensive review of studies on the limits of bone conduction through the head and made further measurements of the attenuation provided by deeply inserted earplugs and by earmuffs and a helmet. Ravicz and Melcher (2001) made additional estimates of the body conduction threshold over a limited frequency range.

The aim of the work reported here was to build on the current understanding of the bone conduction transmission paths and to evaluate the effectiveness of different hearing protection components in providing protection against bone-conducted sound.

2.0 METHODS

2.2 Head Simulator

2.2.1 Need for the Simulator

Measurements of the bone conduction transmission paths in human subjects are limited by the need to make non-invasive measurements and by the difficulty in separating psycho-acoustic responses to air- and bone-conducted sound. Studies on animal models and cadavers have a limited test window that hinders detailed long-term investigations of component performance. In order to overcome these limitations, we developed an instrumented head simulator that reproduced the dynamics of a human head. We validated the simulator

against the human and cadaver mechanical impedance data reported in the literature. We then measured the response of the head to a sound field. Once validated, the simulator provided a valuable test platform for repeat measurements of component effectiveness.

2.2.2 Simulator Construction

The head simulator was built up from a dry human skull. Stages of the build processes are shown in Figure 2. A triaxial accelerometer was bolted onto the right mastoid bone, and uni-axial accelerometers were bolted onto the left mastoid and also onto the left and right interior temporal bones. The mastoid accelerometers were aligned in the transverse direction, and the temporal bone accelerometers were aligned in the axial direction. The skull bones were knitted together using a low-viscosity epoxy (Gougeon WEST System #105 Resin & #206 Hardener). The brain, eyes, nose, and tongue organs and some jaw and neck muscles were simulated by balloons filled with Silicone Dielectric Gel (Dow Corning 3-4150), which set with a consistency and density similar to that of the organs being simulated. The silicon replaced gelatine, which was used in earlier models but began to decompose over time. The jaw was tied into place with rubber bands, and a foam pad was placed between the teeth. The skull was covered with 5-mm thick silicone skin tissue, formulated according to ANSI S12.42-1995. The skin was held in place and tensioned with elastic cloth tape. The external skin layer was simulated by two layers of balloons, stretched tightly over the head. The skull was then inverted and filled with silicon oil (Dow Corning 510) to simulate the cerebrospinal fluid (CSF). Earlier versions of the simulator had used water, and then a dilute solution of hydrogen peroxide, to simulate the CSF, but these solutions caused the bone and other materials to decompose over time. Before making this substitution, we determined the difference between the dynamics of water-soaked bone samples and those of bone samples soaked in silicon oil. Our results showed that the water softened the bone, lowering its natural frequency by 10% compared to dry bone. This result agrees with that reported by Khalil and Viano (1979). The natural frequency of the silicon-soaked bone was 5% lower than that of dry bone, a shift that can be attributed to the increased mass of the soaked sample. As these differences are within the skull-to-skull variability that might be expected, we chose to use the silicon fluid because of its superior preservative and dielectric properties, which significantly increased the shelf life of the skull simulator.



Figure 2. Creare Head Simulator. Left: dry skull with accelerometers mounted on the mastoid bones and on the interior temporal bones. Center: jaw added and organs simulated by latex balloons filled with silicone. Right: tissue simulated by silicone, muscle tension by elastic tape, skin simulated by balloons, remaining cavities filled with silicone oil to simulate cerebrospinal fluid.

2.2.3 Driving Point Impedance Tests

Driving point impedance tests were conducted using a B&K Type 4190 shaker with an impedance head attached (Type 8000). The skull was held against the impedance head with a 2 to 6 lb. force provided by a latex band as shown in Figure 3. Signals from the impedance head (force and acceleration) and from the skull-mounted accelerometers were recorded with the skull driven at the forehead and at the mastoid. Impedance was expressed as velocity divided by force, with velocity determined from the measured accelerations assuming a sinusoidal response. The application force had a minor effect (less than 10%) on the measured driving point impedance and a negligible effect on the response of the bone-anchored accelerometers.

2.2.4 Tests in the Sound Field

The response of the head in a sound field was measured in Creare's acoustic test facility, a 9' by 7' by 7' hemi-anechoic chamber. The head simulator was inverted and suspended in front of a single speaker as shown in Figure 4. The sound field in the head mounting location was carefully mapped and found to be uniform to within 2 dB over a frequency range from 250 Hz to 10 kHz. The response was expressed as acceleration divided by sound pressure level. The latter was measured by a reference microphone positioned adjacent to the head. The head simulator was then fitted with various hearing protection components, and the vibration attenuation was determined by comparing the measured response to that recorded for the bare head.



Figure 3. Driving Point Impedance Test Setup. The head simulator is held against a shaker using latex bands.



Figure 4. Head Simulator Mounted in the Acoustic Test Facility. Simulator is inverted and suspended approximately 1 m from the sound source.

2.3 Human Subject Tests

Human subject tests were carried out with volunteer subjects. All test protocols were reviewed by the local Dartmouth-Hitchcock Medical Center Institutional Review Board. Subjects were healthy males and females between 18 and 50 years of age with normal hearing (less than 15 dBA hearing loss for the frequency range 500 Hz to 6000 Hz) and a normal otoscopic exam.

2.3.1 Human Subject Driving Point Impedance Tests

Driving point impedance tests similar to those conducted on the head simulator were also conducted with human subjects using a B-70 bone oscillator in series with the B&K Type 8000 impedance head. Two subjects were tested and similar responses were obtained from each.

2.3.2 Human Subject Tests in the Sound Field

HPD component performance was measured using a modified Real Ear Attenuation at Threshold (REAT) technique. The technique is defined by ANSI Standard S12.6-1997. HPD attenuation is determined from hearing threshold measurements with and without the hearing protection in place. Pulses of third-octave noise are presented to the subject in a diffuse sound field. The modified technique employed in this study used a directional hemi-anechoic sound field instead of a diffuse field. This was primarily due to the facility available, but it did allow the directional performance of the HPD to be determined. Subjects were fitted with deeply inserted “Grande™” earplugs from E.A.R for the first level of protection. The helmet included Howard Leight Industries’ “Thunder 29” earmuffs for the second level of protection. The helmet shell, fitted with an edge seal, inner liner, and face shield, provided the third level of protection.

2.3.3 Head Isolation Tests

The goal of the head isolation test apparatus was to expose a subject’s body to sound, while isolating their head and ears from this sound. This was done by fitting the subject with triple hearing protection (earplugs, earmuffs, and a sound-attenuating helmet) and then placing them in a sound-attenuating box with their head protruding, as shown in Figure 5. A speaker capable of producing 130 dB SPL was mounted inside the box. Before fitting the subject in the box, the attenuation provided by the triple hearing protection was measured in the sound room using the modified REAT technique described above. The attenuation provided by the box was measured directly by subtracting the average sound level from a sound field survey inside the box from the sound level measured by a reference microphone adjacent to the subject’s head outside the box. The perceived attenuation of the sound presented inside the box was then measured by a threshold test. A valid measurement of the body-conducted sound threshold is obtained if the attenuation of sound perceived by the subject was less than the sum of that provided by the box and the helmet together. If this is the case, the perceived sound must be coming via a body-conducted sound route, as the attenuation is less than the measured bypass route through the box and the HPD.

3.0 RESULTS

3.1 Head Simulator Validation

The fidelity of the head simulator was validated by comparing driving point impedance measurements from the forehead and mastoid to similar measurements on human subjects and to results reported in the literature. The results, shown in Figure 6, are in very good agreement, indicating that the simulator responds in a similar manner to a human head. The forehead impedance measurements were made using a B-70 bone oscillator, with the same apparatus being used for both the head simulator and for human subjects. Other measurements on the head simulator used a B&K shaker, which provided a larger excitation. The results compare well with the non-skin penetrating data of Hakansson et al. (1986), who made measurements on the mastoid of human subjects and with the impedance specified in the standard for artificial mastoids (IEC 373:1990). The data are similar in form but slightly lower than those of Smith and Suggs (1976), who obtained non-skin penetrating impedance measurements for both frontal and occipital locations.

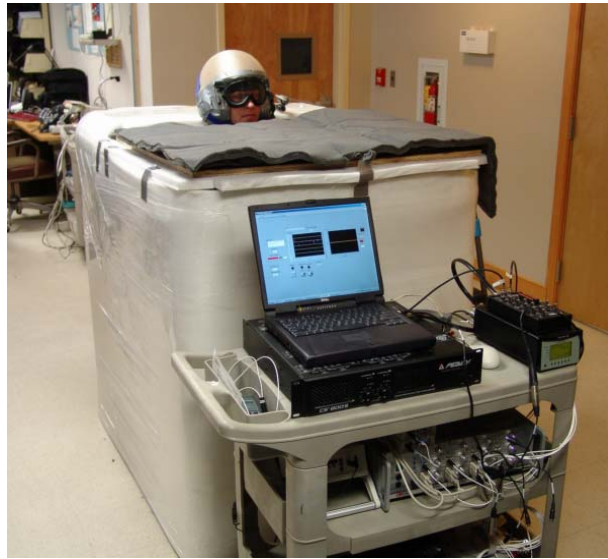


Figure 5. Head Isolation Experiment Setup.

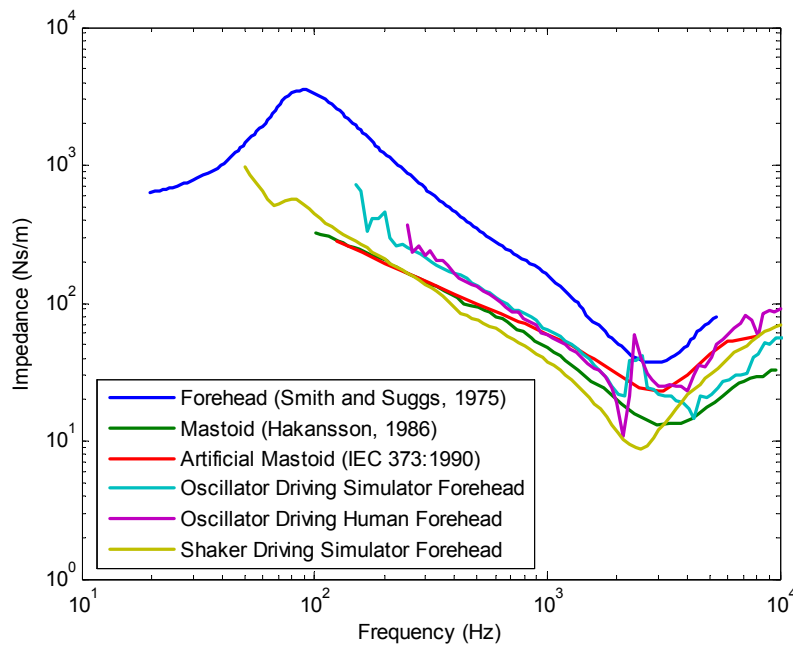


Figure 6. Driving Point Impedance Data from the Head Simulator Compared with Data from the Literature. Force and acceleration are measured at the driving point.

Impedance results from the bone-anchored accelerometers mounted in the mastoid of the head simulator are shown in Figure 7. The measurements by Stalnaker et al. (1971) from a bone-anchored accelerometer mounted in a cadaver mastoid are also included in the figure, as are measurements by Hakansson et al. (1986) from an accelerometer fixed to a titanium implant for a bone-anchored hearing aid. The impedance measured at the bone-anchored sites is higher than that measured at the skin, and there is significant variability between

studies and between measurement sites within a study. Both the location and the magnitude of the anti-resonance and the resonance were dependent on the forcing and measurement locations. However, the general agreement between the form and magnitude of the response from the head simulator compared with that presented in the literature provides confidence that the simulator has a similar response to that of a human head.

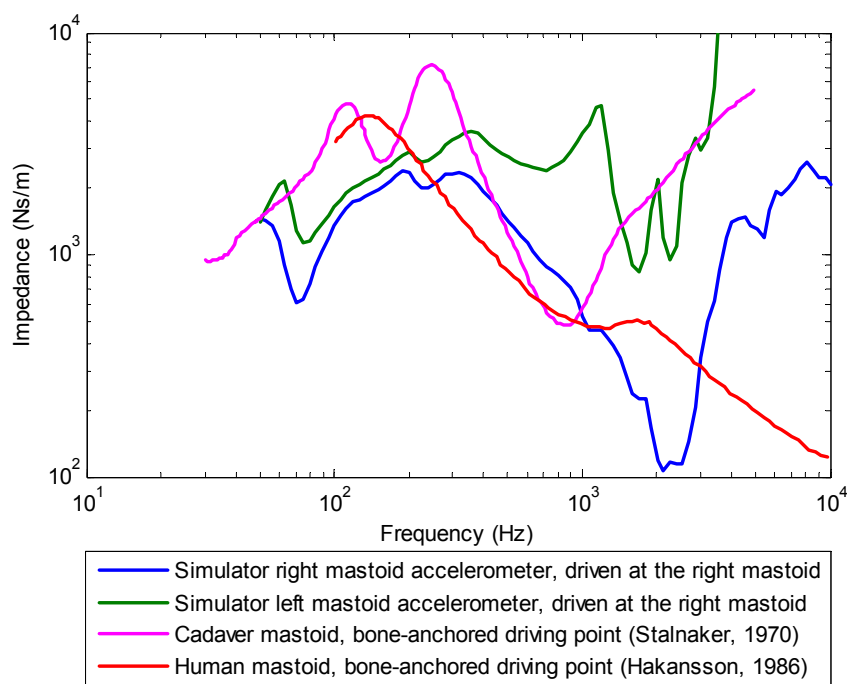


Figure 7. Driving Point Impedance Data from the Head Simulator Compared with Data from the Literature. Driven at the mastoid and acceleration measured with bone-anchored accelerometers.

3.2 Driving Point Response

The modal behaviour of the head can be understood by considering the magnitude and phase of the driving point impedance measurements. The response of the dry skull and of the reconstituted head simulator when driven at the right mastoid is shown in Figure 8. The mastoid bone accelerometers were mounted facing outwards, opposing each other. Below the first resonant frequency, the skull moves as a rigid body, and the phase difference between the z-axis of the right mastoid accelerometer (tri-axial) and the signal from the left mastoid accelerometer (uni-axial) is approximately 180 degrees. At the frequency of the first anti-resonance of the dry skull (800 Hz), the phase difference moves to zero, indicating the bones are vibrating in opposite directions, and the skull is entering the first compression mode. The dry skull resonance occurs at 1000 Hz and is followed by more modes and complicated phase transitions at higher frequencies. The largest response (impedance minimum) occurs at 2 kHz. The increased damping present in the head simulator smoothes out the sharp phase transitions seen in the dry skull data, but the same general trends are apparent. The low-frequency response of the skull and head are similar to that of two-degree-of-freedom systems, which exhibit a 180-degree phase shift at the first anti-resonance. Above the first resonant frequency (approximately 1000 Hz for the dry skull), the phase relationship changes continually, and the skull exhibits many vibration modes.

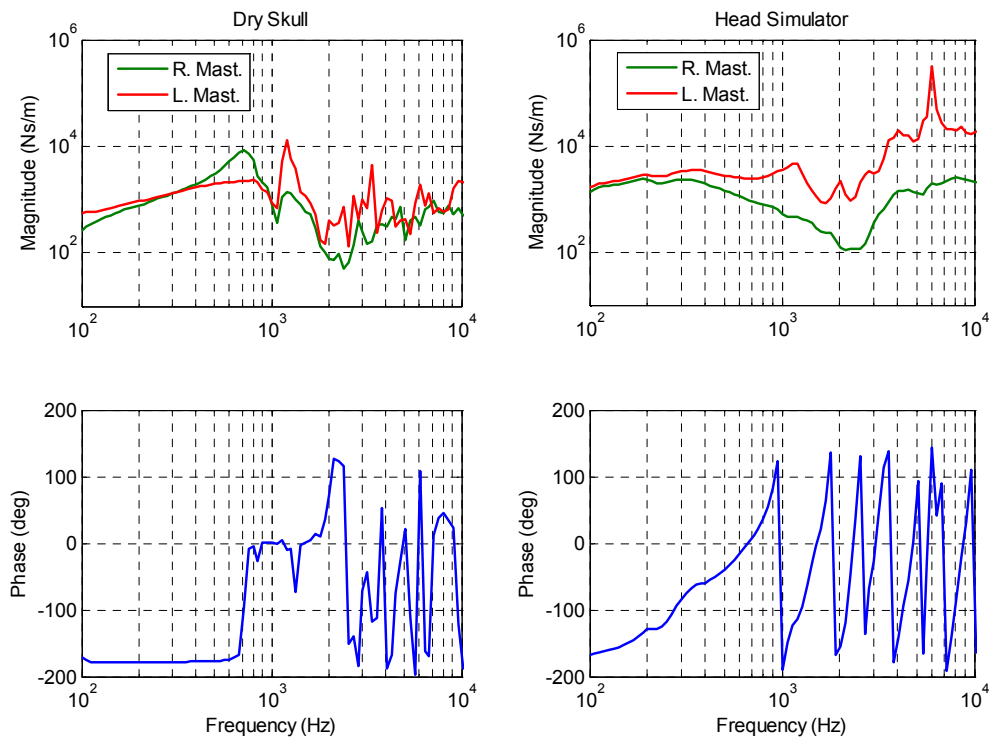


Figure 8. Driving Point Response. Dry skull response shown on the left, head simulator response shown on the right. Driven at the right mastoid. Results for the bone-anchored accelerometers mounted on the right and left mastoid are shown in the upper plots. The relative phase between the two accelerometers is shown in the lower plots.

3.3 Sound Field Excitation

The response of the head simulator to forcing from a sound field is shown in Figure 9 and Figure 10, with the head positioned facing the sound source and facing to the left of the sound source respectively. Data for each of the mastoid and temporal bone accelerometers are plotted in the figures. The acceleration values have been normalized by the forcing sound pressure level measured by a reference microphone adjacent to the head. Results for four separate tests are plotted to show test repeatability. Both the mastoid and the temporal bone accelerometers exhibit a rising response, which reaches a maximum at approximately 2 kHz. A complex response with many modes is seen at higher frequencies. Note that some directional effects can be seen below 500 Hz, but the responses are largely independent of orientation to the sound field above this frequency. For instance, the response of the uni-axial left mastoid accelerometer is higher when the helmet is oriented sideways, aligning the accelerometer axis with the direction of the sound forcing. The temporal bone accelerometers have a higher response when the head is facing the sound field, aligning these accelerometers with the direction of the sound forcing. The right mastoid acceleration is the resultant acceleration measured by the triaxial accelerometer, and as such, it shows little dependence on orientation. These data support the results from the driving point tests, which indicated that the head was vibrating as a rigid body for frequencies below 1 kHz and transitions to distortional modes of vibration at higher frequencies.

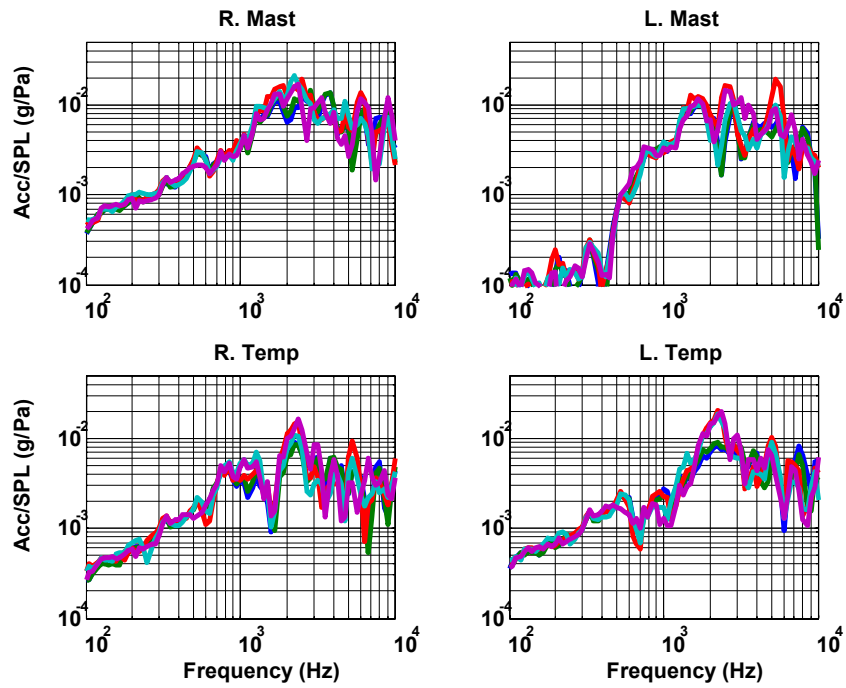


Figure 9. Head Response to Forcing from a Sound Field. Head simulator was placed facing the speaker in a hemi-anechoic chamber.

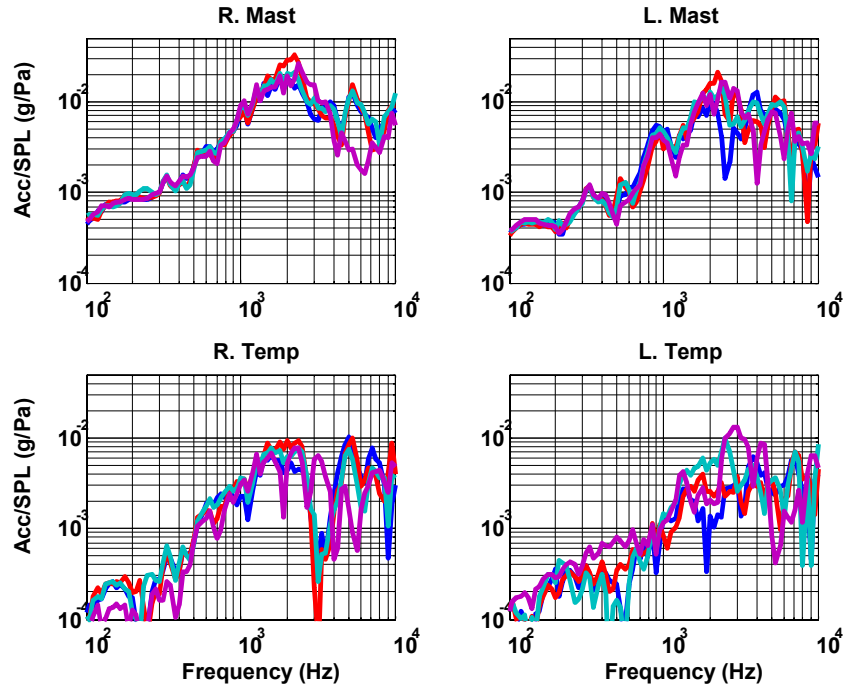


Figure 10. Head Response to Forcing from a Sound Field. Head simulator was placed facing to the left of the speaker in a hemi-anechoic chamber.

3.4 HPD Performance on Head Simulator

The complex nature of the high-frequency vibration would make it difficult to tune out or cancel the vibrations. The results of limited experiments with added damping and with active vibration cancellation supported this conclusion. Therefore, our focus was on attenuating the bone conduction transmission paths by shielding the head from the sound field. Shielding is achieved by wearing a helmet as a third layer of hearing protection, in addition to earplugs and earmuffs. A helmet was fabricated using rapid prototyping techniques for this study. The helmet, similar to that shown in Figure 11, comprised an outer shell, a foam liner, a sealed foam edge seal, and a face shield. The vibration attenuation provided by the helmet components was measured by fitting the helmet onto the head simulator and measuring the bone vibration with the head positioned in different orientations to the sound field. Representative results are plotted in Figure 12 and in Figure 13. The addition of earmuffs has a minimal effect on the head vibration, with the attenuation remaining below 5 dB for all frequencies. The same was also true for the foam liner, although these results are not included in the plot. The addition of a hard shell sealed to the head provided an approximately 10-dB increase in attenuation in the critical bone conduction frequency range around 2 kHz for sound directed from the back, while a face shield was required to give equivalent attenuation of sound directed from the front. At higher frequencies, the attenuation approached 20 dB. However, at frequencies below the first resonance where the head is vibrating as a rigid body, the helmet actually amplified the skull vibrations.



Figure 11. Hearing Protection Helmet. Helmet includes a hard shell, a foam liner, a sealed foam edge roll, earmuffs, and face shield.

Hearing Protection for Bone-Conducted Sound

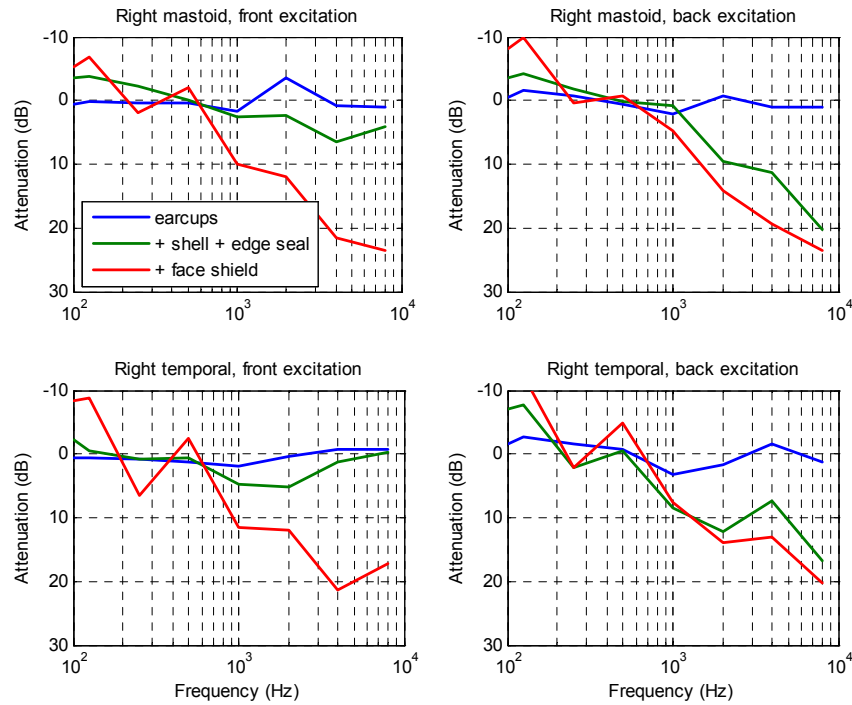


Figure 12. Vibration Attenuation Provided by Helmet Components on the Head Simulator in a Directional Sound Field. Head is oriented towards the sound field in the plots on the left, and away from the sound field in the plots on the right.

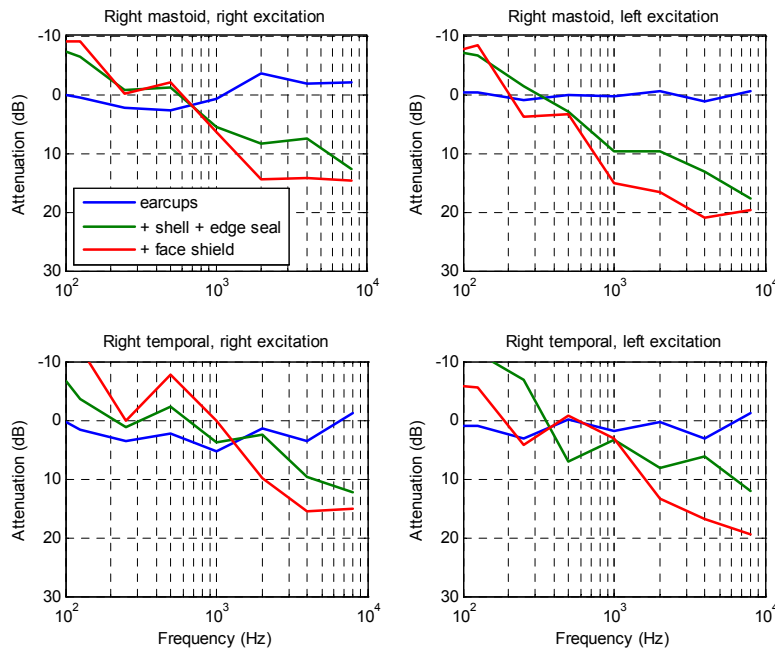


Figure 13. Vibration Attenuation Provided by Helmet Components on the Head Simulator in a Directional Sound Field. Head is oriented towards the sound field in the plots on the left, and away from the sound field in the plots on the right.

3.5 HPD Performance on Human Subjects

Various hearing protection configurations were also tested on human subjects to confirm the results from the simulator tests. Measured attenuation for plugs alone (single protection), plugs and muffs (double protection), and plugs, earmuffs, and helmet (third level) are shown in Figure 14. The helmet provides a significant increase in attenuation at frequencies above 1 kHz. At the lower frequencies, triple protection is no better than double protection, and at some frequencies may be worse. At higher frequencies, triple protection provides significantly greater attenuation. At 2 kHz, where the bone conduction response to sound is the greatest, the bone conduction limit is 40 dB, as represented by the limited double hearing protection attenuation. The triple protection provided by a helmet increases the mean attenuation to 55 dB. Therefore, the helmet is providing a 15-dB increase in attenuation. If the double protection is assumed to attenuate the air-conducted sound beyond the bone conduction limit, then the attenuation of bone-conducted sound is represented by the difference between the double protection attenuation and the triple protection attenuation (i.e., between plugs and muffs and plugs, muffs, and shell). A comparison of Figure 14 with Figure 12 shows that the frequency-dependent magnitude of the bone conduction attenuation provided by the helmet on human subjects is similar to the vibration attenuation provided by the helmet fitted to the head simulator. This result further confirms the value of the head simulator as a tool for hearing protection design and suggests that bone vibration is an adequate indicator of bone-conducted sound transmission.

The incremental increases in attenuation provided by partial coverage goggles or a full coverage face shield are shown in Figure 15. These data further support the results from the head simulator, which showed a similar increase in attenuation when the face shield was introduced.

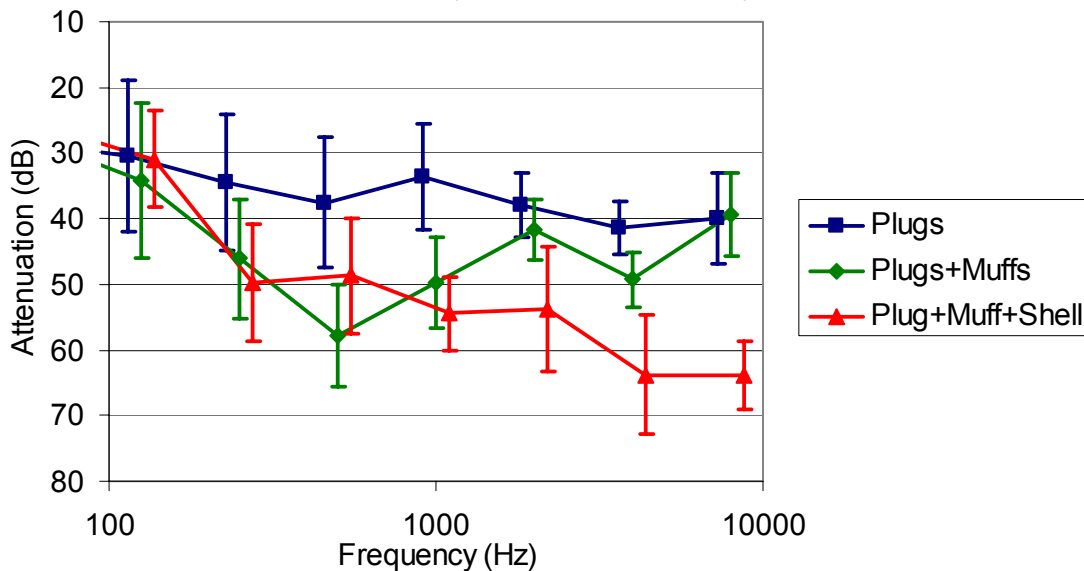


Figure 14. Attenuation Provided by Hearing Protection Components on Human Subjects. Results are the ensemble average of 8 subjects. Modified REAT protocol used (subjects facing towards directional sound field, pure tones, hemi-anechoic chamber). Error bars show ± 1 standard deviation (note points have been offset to distinguish the error bars).

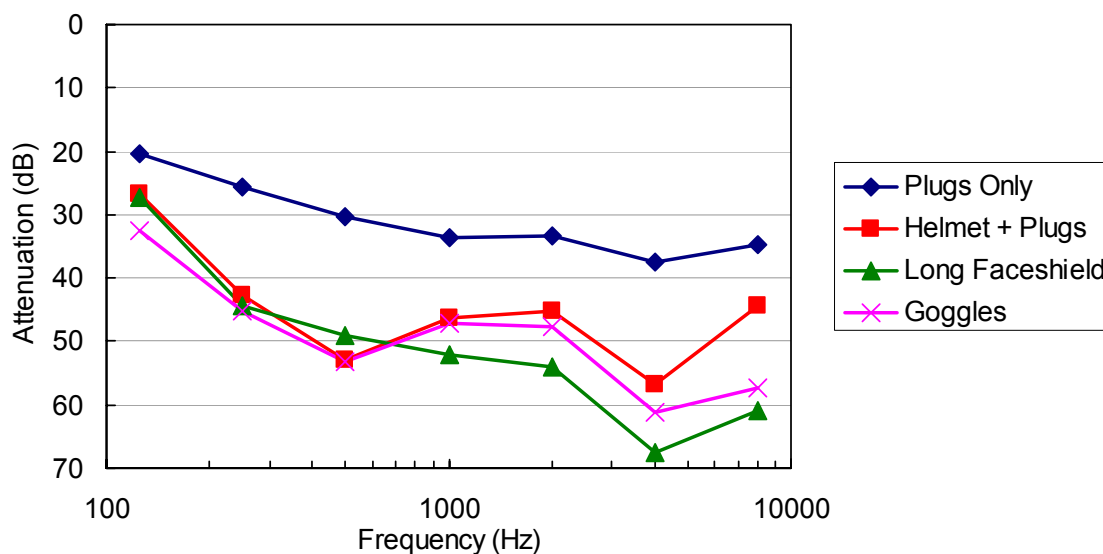


Figure 15. Attenuation Provided by Hearing protection Components on Human Subjects. Results are the ensemble average of 7 subjects. Modified REAT protocol used (subjects facing towards directional sound field, pure tones, hemi-anechoic chamber).

3.6 Head Isolation Tests

The body conduction thresholds measured for six test subjects are shown in Figure 16. The threshold levels increase with frequency from approximately 40 dB at 63 Hz to 80 dB at 8 kHz. There is reasonable consistency between the test subjects. These results are in general agreement with those of Ravicz and Melcher (2001) who measured a body conduction threshold of approximately 60 dB at 1 kHz.

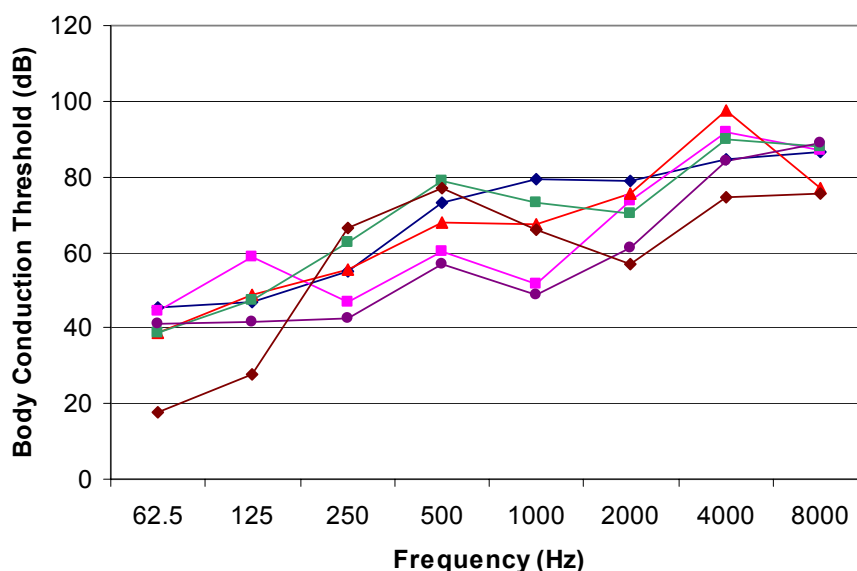


Figure 16. Body Conduction Thresholds. Results for six subjects shown.

The validity of the results may be checked by testing whether the difference between the measured body conduction attenuation is significantly different to that of the bypass path (hearing protection and box attenuation). A statistical *t* test showed a highly significant ($P = 0.01$) difference in five of the eight frequencies tested (250 Hz, 1 kHz, 2 kHz, 4 kHz, and 8 kHz). This significance is apparent in the summary plot shown in Figure 17, where the error bars correspond to a standard error with a 95% confidence interval. The helmet attenuation is also included in this plot.

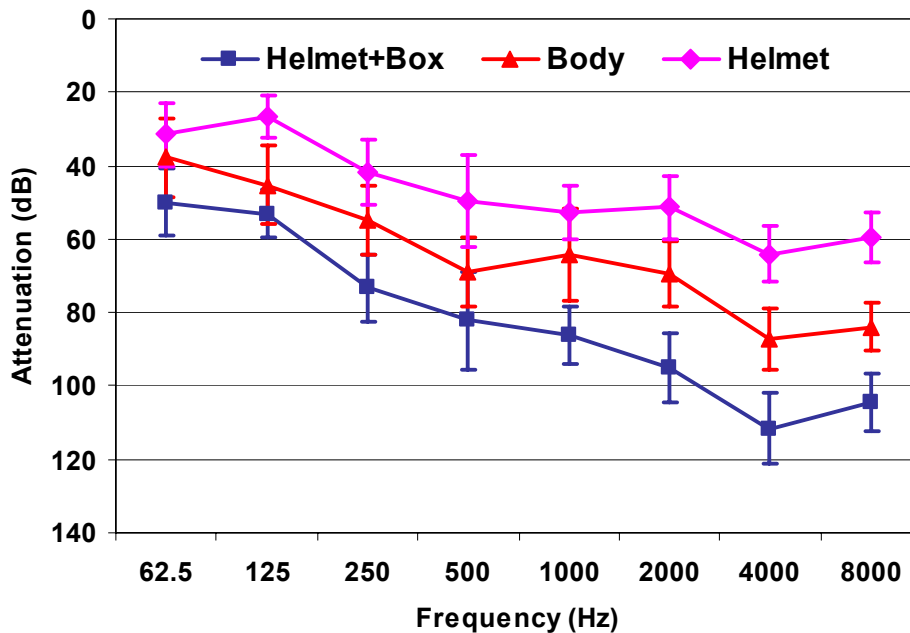


Figure 17. Summary Plot. Mean data for all subjects is shown with standard errors representing 95% confidence intervals.

5.0 SUMMARY AND CONCLUSIONS

An investigation into bone-conducted transmission paths and the effectiveness of hearing protection devices against these paths was conducted using human subjects and a head simulator. The response of the head simulator was validated by comparing its driving point impedance with results from tests on human subjects and with results reported in the literature. The vibration response of the head simulator in a sound field was then measured. The response was greatest above the first resonance in the frequency range between 2 kHz and 3 kHz, which is the frequency range where bone conduction transmission limits the attenuation of hearing protection devices. The modal behavior of the skull is complicated and bone vibration is most effectively reduced by shielding the head from the sound field with a helmet and a face shield. Measurements with the head simulator showed that shielding can provide between 10 and 20 dB of attenuation of bone vibration above 1 kHz. Measurements on human subjects showed a similar increase in sound attenuation beyond the head conduction limit represented by double protection (earplugs and earmuffs). If the head were completely shielded from the sound field, the attenuation would be limited by body conduction. Measurements of the body conduction limit found that the limit increases from 40 dB at 63 Hz to 80 dB at 8 kHz. The relative head and body conduction limits measured in this study are summarized in Figure 18.

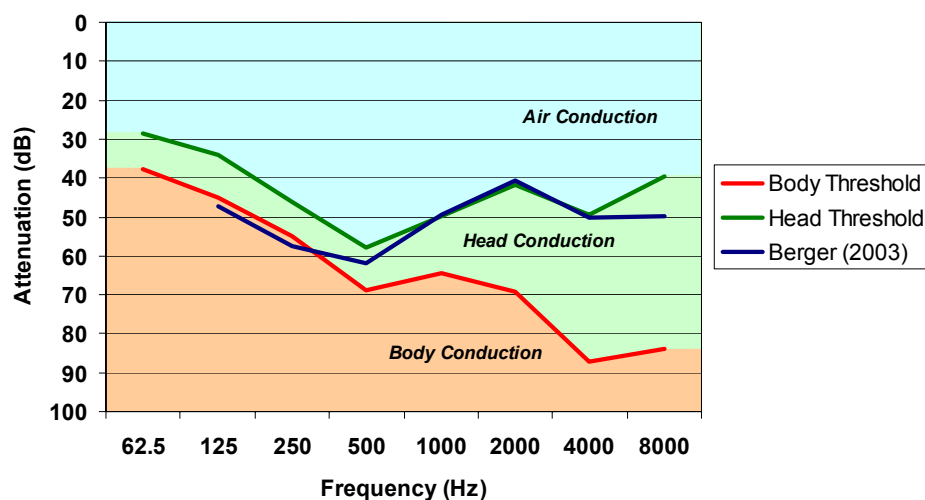


Figure 18. Head and Body Thresholds for Sound Conduction.

6.0 REFERENCES

- [1] Berger, E.H. and Kieper, J.E., "Hearing Protection: Surpassing the Limits to Attenuation Imposed by the Bone-Conduction Pathways," *J. Acoust. Soc. Am.*, Vol. 114, No. 4, Pt 1, Oct 2003, pp. 1955–1967.
- [2] Berger, E.H. and Kerivan, J.E., "Influence of Physiological Noise and the Occlusion Effect on the Measurement of Real-Ear Attenuation at Threshold," *J. Acoust. Soc. Am.*, Vol. 74, No. 1, July 1983, pp. 81–94.
- [3] Hakansson, B. and Carlsson, P., "The Mechanical Impedance of the Human Head with and without Skin Penetration," *J. Acoust. Soc. Am.*, Vol. 80, No. 4, 1986, pp. 1065–1075.
- [4] Khalil, T.B., and Viano, D.C., "Experimental Analysis of the Vibrational Characteristics of the Human Skull," *J. Sound and Vibration*, Vol. 63, No. 3, 1979, pp. 351–376.
- [5] Ravicz M.E., and Melcher, J.R., "Isolating the Auditory System from Acoustic Noise During Functional Magnetic Resonance Imaging: Examination of Noise Conduction through the Ear Canal, Head, and Body," *J. Acoust. Soc. Am.*, Vol. 109, No. 1, Jan 2001, pp. 216–241.
- [6] Smith, J.B. and Suggs, C.W., "Dynamic Properties of the Human Head," *J. Sound and Vibration*, Vol. 48, No. 1, 1976, pp. 35–43.
- [7] Sohmer, H., Freeman, S., Geal-Dor, M., Adelman, C. and Savion, I., "Bone Conduction Experiments in Humans – a Fluid Pathway from Bone to Ear," *Hearing Research*, Vol. 146, No. 1-2, 2000 pp. 81–88.
- [8] Stalnaker, R.L., Fogler, J. L. and McElhaney, J. H., "Driving Point Impedance Characteristics of the Head," *J. Biomechanics*, Vol. 4, 1971, pp. 127–139.
- [9] Tonndorf, J., "Bone Conduction. Studies in Experimental Animals," *Acta Oto-Laryngol.*, Suppl. 213, 1966, pp. 1–132.

ACKNOWLEDGEMENT OF SUPPORT AND DISCLAIMER (MAY 1995)

This material is based upon work supported by the U.S. Department of the Navy under Contract No. N00421-02-C-0266 and by the U.S. Air Force under Contract No. F49620-03-C-0008. The support of the Navy technical monitor, Mr. Jim Wilt, and of the Air Force technical monitor, Mr. Willard Larkin, is gratefully acknowledged. Our collaboration with the Dartmouth Engineering School including Professor Laura Ray, Professor Bob Collier, and Mr. Matt Maher is also gratefully acknowledged.

Any opinions, findings, and conclusions or recommendations expressed in this material are those of the author(s) and do not necessarily reflect the views of the U.S. Department of the Navy or the U.S. Air Force.

